Int. J. Heat Mass Transfer. Vol. 10, pp. 37–59. Pergamon Press 1967. Printed in Great Britain

STUDY ON FORCED CONVECTIVE HEAT TRANSFER IN CURVED PIPES (2ND REPORT, TURBULENT REGION)

YASUO MORI and WATARU NAKAYAMA
Department of Mechanical Engineering, Tokyo Institute of Technology

(*Received* 22 *February* 1966)

Abstract—For this paper the effect of curvature on heat transfer for fully developed turbulent flow in curved pipes on the condition of constant heat flux was studied theoretically and experimentally. In the analysis, a boundary layer is considered to exist along the pipe wall. Local shear stress and local heat flux at the wall are given on the basis of reducing the resistance (λ_s) and the Nusselt number (Nu_s) formula for straight pipes to the local relation of friction and heat transfer. When the formulae for straight pipes are given as $\lambda_s \propto Re^{-1/m}$ and $Nu_s \propto Re^{(m-1)/m}$, it is shown that the dynamic similarity and also the similarity for heat transfer in curved pipes depend upon $Re(a/R)^{m/2}$.

The resistance coefficient and the Nusselt number for curved pipes are obtained by putting $m = 4$ or $m = 5$.

The Nusselt numbers obtained from measurement of the velocity and temperature distributions in the air flow through the curved pipes of $R/a = 40$ and 18·7 are in good agreement with the theoretical results.

NOMENCLATURE

A, w_1 at the centre of a cross section perpendicular to the pipe axis;
A', g_1 at the centre of a cross section perpendicular to the pipe axis;
a, radius of the pipe;
C, coefficient $= -(\partial P/H\partial\theta)$;
c_p, specific heat of fluid at constant pressure;
D, dimensionless velocity of the secondary flow in the flow core;
$f_{\theta\eta}$, $\equiv (a^2/\nu^2)(\tau_{\theta r}/\rho)$;
$f_{\theta\psi}$, $\equiv (a^2/\nu^2)(\tau_{\theta\psi}/\rho)$;
G, $\equiv T_w - T$;
g, $\equiv G/\tau a$;
g_m, $\equiv (T_w - T_m)/\tau a$;
$\check{g}$, g in a straight pipe expressed by the $1/n_0$ power law;
k, heat conductivity of fluid;
M, exponent of $w_{1\delta}$ [equation (18)];
m, constant giving exponent of Re in the formula for λ_s [equation (9)] or Nu_s [equation (68)];
Nu, Nusselt number, $\equiv [2aQ_{wm}/k(T_w - T_m)]$;
n, constant giving g in the boundary layer [equation (81)];
n_0, constant giving g in a straight pipe [equation (61)];
P, $\equiv (a^2/\nu^2)(p/\rho)$;
Pr, Prandtl number, $\equiv \rho c_p \nu/k$;
p, pressure;
Q_η, Q_ψ, heat flux in the fluid;
Q_w, heat flux at the wall to the fluid per unit area and unit time;
q_η, $\equiv Q_\eta/k\tau$;
q_ψ, $\equiv Q_\psi/k\tau$;
q_w, $\equiv Q_w/k\tau$;
R, radius of curvature of the pipe axis;
Re, Reynolds number, $\equiv (2aW_m/\nu)$;
r, co-ordinate in radial direction in the cross section;
T, time-averaged temperature;
T_m, mixed mean fluid temperature;
T_w, wall temperature;
U, radial component of time-averaged velocity;
u, $\equiv Ua/\nu$;

V, circumferential component of time-averaged velocity;
v, $\equiv Va/\nu$;
v^*, circumferential component of dimensionless friction velocity;
W, axial component of velocity;
w, $\equiv Wa/\nu$;
W_m, mean velocity;
w^*, axial component of dimensionless friction velocity;
$\check{w}$, dimensionless velocity in a straight pipe or resultant velocity formed by v and w;
$\check{w}^*$, dimensionless friction velocity, $\equiv (a/\nu)\sqrt{(\tau_w/\rho)}$;
Y, coefficient given by equation (67).

Greek symbols

α, proportional coefficient in the formula for λ_s [equation (9)];
α_c, proportional coefficient in the formula for λ_c [equation (36)];
β, proportional coefficient in the formula for Nu_s [equation (68)];
γ_0, constant in equation (54);
Δ, coefficient of correction term, [Suffix (A', g_m, Nu, λ) denotes the correction term for them];
δ, thickness of the boundary layer divided by a;
$\hat{\delta}_m$, coefficient in equation (34) giving δ_m;
ϵ, eddy diffusivity;
H, $\equiv R/a$;
η, $\equiv r/a$;
θ, axial co-ordinate;
κ, exponent of Pr in the formula for Nu_s [equation (68)];
λ, resistance coefficient, $\equiv [(-\partial P/R\partial\theta)(2a/\frac{1}{2}\rho W_m^2)]$;
ν, kinematic viscosity;
ξ, $\equiv 1-\eta$;
ρ, density;
τ, temperature gradient along the pipe axis;
τ_w, frictional stress at the wall;
$\tau_{\theta r}$, $\tau_{\theta\psi}$, shear stresses in the direction of pipe axis;
ψ, circumferential co-ordinate in the cross section.

Subscripts

1, value in the flow core region;
b, value at the boundary between buffer layer and turbulent core in a straight pipe;
c, curved pipe;
f, value at the position where v in the boundary layer becomes maximum;
m, mean value around the periphery ($\psi = -\pi \sim \pi$), (except g_m, T_m, W_m);
s, straight pipe;
δ, value at $\xi = \delta$.

INTRODUCTION

IN A CURVED pipe, the centrifugal force of a flowing fluid produces a pressure gradient in a cross section. This pressure gradient yields a pair of secondary flows. The secondary flows cause a larger amount of pressure drop or heat-transfer rate than those for a straight pipe. To evaluate the effect of curvature on the heat-transfer rate is of fundamental importance for the design of heating or cooling coils and for other industrial requirements.

In the previous paper [1], heat transfer in a fully developed laminar flow is discussed. The velocity and temperature distributions in the curved pipe are measured. These profiles show that a thin boundary layer is formed along the pipe wall. Theoretical analysis is done by dividing the flow and temperature field into a core region and the boundary layer. The formulae of Nusselt numbers applicable in a fairly wide range of Dean numbers [$K \equiv Re\sqrt{(a/R)}$] are suggested.

For a turbulent flow, the empirical formula of Jeschke [2] has been quoted in many books [3]. Others can be found in the reports of Pratt [4], Seban and McLaughlin [5], Rogers and Mayhew [6]. These results have been derived from experimental data utilizing a few cases of curva-

ture to pipe radius ratio. The fluid is air or water. The heat-transfer rate is obtained by the measurements of the bulk mean temperature at the fixed two stations and the total heat flux from the pipe wall to the fluid between the stations.

This method is conventional for heat-transfer experiments in pipes or conduits, but provides little information about heat-transfer processes inside the fluid. The effect of curvature is far less evident in a turbulent flow than in a laminar flow. Therefore, in order to establish a general correlation, an amount of data from different cases of radius ratio and a high degree of accuracy in experiments are required. It is thought that there should be a shorter way to approach the general formula of Nusselt numbers. The most effective way is to examine the velocity and temperature distributions inside a pipe theoretically and experimentally, and show how the Nusselt number is affected by curvature through the distortion of distribution profiles. Up to the present, theoretical study of the problem has scarcely been made.

The only theoretical analysis of the flow resistance in curved pipes was done by Ito [7]. The boundary layer concept is employed. The resistance formula is given in an asymptotic form which gets nearer to the empirical correlation in the region of large Reynolds numbers, like Adler's analysis for laminar flow [8]. However, there is a difference between the theoretical results and the experimental results over the practical range of Reynolds numbers. The procedure of calculation is so complex that it does not fit the purpose of applying the analysis of the flow field to the heat-transfer problem.

In this report, variations of physical properties with temperature are not taken into consideration. The theoretical analysis for a turbulent flow in curved pipes is made in a manner which is rather simple and suitable for the discussion of heat transfer. Heat transfer in a fully developed temperature field on the condition of constant heat flux is discussed theoretically. The experiments were made to investigate the velocity and temperature distributions in air flow. The Nusselt numbers were also obtained as the experimental results.

THEORETICAL ANALYSIS OF THE FLOW IN A CURVED PIPE

In the present paper, the far side of the wall from the center of curvature is called the outer wall, and the near side is called the inner wall. In a curved pipe, the fluid in the central part is driven toward the outer wall by centrifugal force. The fluid near the wall flows along the wall surface to the inner wall. Thus in the pipe the regular secondary flow forms a pair of vortices in a cross section. When the balance of forces in the direction of the pipe axis is considered, it is noticed that stress caused by the secondary flow shares with other kinds of stress the role of counter force to the pressure gradient.

The system of co-ordinates is taken as shown in Fig. 1. The shear stresses in the direction of

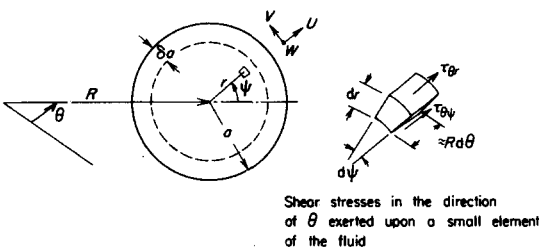

FIG. 1. System of co-ordinates.

the axis (θ) are $\tau_{\theta r}$, $\tau_{\theta\psi}$. All quantities are expressed in non-dimensional form, as follows:

$$\eta = r/a, \qquad H = R/a, \qquad u = Ua/\nu,$$

$$v = Va/\nu, \qquad w = Wa/\nu, \qquad P = \left(\frac{a^2}{\nu^2}\right)\left(\frac{p}{\rho}\right),$$

$$f_{\theta\eta} = \left(\frac{a^2}{\nu^2}\right)\left(\frac{\tau_{\theta r}}{\rho}\right), \qquad f_{\theta\psi} = \left(\frac{a^2}{\nu^2}\right)\left(\frac{\tau_{\theta\psi}}{\rho}\right).$$

When the flow is steady and fully developed, the pressure gradient along the pipe axis is constant.

The constant in a dimensionless form is written as $C \equiv -(\partial P/H\partial\theta)$. It is assumed that $r/R \ll 1$, and all geometrical small terms are omitted. Then, the force balance equation is expressed as follows:

$$\frac{\partial}{\eta\partial\eta}(\eta f_{\theta\eta}) + \frac{\partial f_{\theta\psi}}{\eta\partial\psi} = -C. \tag{1}$$

The shear stresses are

$$\left.\begin{aligned} f_{\theta\eta} &= \frac{\partial w}{\partial\eta} - uw - \overline{u'w'} \\ f_{\theta\psi} &= \frac{\partial w}{\eta\partial\psi} - vw - \overline{v'w'}. \end{aligned}\right\} \tag{2}$$

In this equation u, v, w are the time-averaged mean-velocity components; u', v', w' are the components of turbulent fluctuation; and $\overline{u'w'}$, $\overline{v'w'}$ are Reynolds stresses.

When the flow is turbulent, a mean velocity is always large enough to produce the secondary flow which shows a remarkable effect in determining the main feature of the velocity distribution. Only the shear stresses uw, vw are supposed to be predominant over a cross section of the pipe except a thin layer along the wall. Hereafter, the region where the stresses caused by the secondary flow are predominant is called a core region. The thin layer next to the wall where all kinds of stresses cannot be ignored is called a boundary layer. The region of the boundary layer is represented by δ which is the dimensionless thickness divided by the pipe radius a.

When the secondary flow is brought into consideration, its appearance is imagined as follows. The fluid in the core region flows towards the outer wall, then enters the boundary layer. There is a return flow toward the inner wall in the layer. The conceivable stream lines are shown in Fig. 2. In these circumstances, the work done by pressure in the direction of the pipe axis (which is called θ-direction) is lost by turbulent and laminar diffusion mainly in the boundary layer. When the pressure gradient in θ-direction is constant, δ representing the thickness of the layer of diffusion is invariable in θ-direction, and varies only in a cross section.

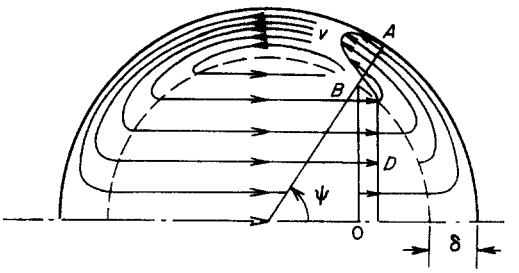

FIG. 2. Secondary flow streamlines.

1. *The velocity distributions in the core region*

In this region the velocity components u, v, w, are denoted by u_1, v_1, w_1 respectively. The shear stresses are expressed by

$$f_{\theta\eta} = -u_1 w_1, \qquad f_{\theta\psi} = -v_1 w_1. \tag{3}$$

The relations between the centrifugal force of fluid and the pressure gradient in a cross section are

$$\frac{w_1^2}{H}\cos\psi = \frac{\partial P}{\partial\eta}, \qquad \frac{w_1^2}{H}\sin\psi = -\frac{\partial P}{\eta\partial\psi}. \tag{4}$$

Elimination of the pressure terms from these equations yields the following relation for w_1:

$$\cos\psi\frac{\partial w_1}{\eta\partial\psi} + \sin\psi\frac{\partial w_1}{\partial\eta} = 0. \tag{5}$$

The equation of continuity is written as

$$\frac{\partial}{\eta\partial\eta}(\eta u_1) + \frac{\partial v_1}{\eta\partial\psi} = 0. \tag{6}$$

The velocity components u_1, v_1, w_1 satisfying equations (5) and (6) are put in the most simple forms as follows:

$$\left.\begin{aligned} u_1 &= D\cos\psi \\ v_1 &= -D\sin\psi \\ w_1 &= A + (C/D)\eta\cos\psi \end{aligned}\right\} \tag{7}$$

where A and D are constants. The secondary flow in the core region is expressed by a uniform flow toward the outer wall.

2. *The shear stress at the wall and the velocity distributions in the boundary layer*

The distance from the wall is denoted by $\xi = 1 - \eta$. As shown in equation (7), the velocity at the edge of the boundary layer ($\xi = \delta$) varies with the angle ψ in a cross section. The characteristics of the flow in the boundary layer are determined by the velocity at $\xi = \delta$. Since the local shear stress at the wall depends on the velocity in the boundary layer, τ_w also varies with ψ. The shear stress τ_w is expressed non-dimensionally by the friction velocity $\check{w}^* = (a/\nu)\sqrt{(\tau_w/\rho)}$.

The circumferential component (ψ-component) of the velocity in the boundary layer v has a distribution like that shown in Fig. 2. The distance from the wall where v becomes the maximum value v_f is denoted by ξ_f.

The axial velocity component w at $\xi = \xi_f$ is written as w_f. The components v_f and w_f form a velocity $\check{w}_f$ as shown in Fig. 3. The relation between $\check{w}^*$, ξ_f and $\check{w}_f$ might be considered to be obtained from the law which describes the relation in a straight pipe between the shear stress at the wall, the distance from the wall and the velocity at the position. The law in regard to a straight pipe may be derived from the resistance formula. The resistance coefficient λ is defined as

$$\lambda = \left(-\frac{\partial p}{\partial z}\right)\frac{2a}{\frac{1}{2}\rho W_m^2} \tag{8}$$

where z is the co-ordinate taken along the pipe axis. We use the suffix s to indicate that the case is one of a straight pipe. The formula for a straight pipe is expressed in general terms as

$$\lambda_s = \alpha\, Re^{-(1/m)} \tag{9}$$

where

$$Re = 2aW_m/\nu.$$

For the appropriate range of Reynolds numbers, α and m are determined in order to approximate the actual relation between λ_s and Re. The commonly used value of m is 4 or 5.

When m is taken as 4, the value of α is 0·316

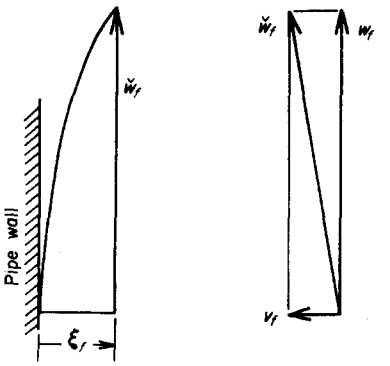

FIG. 3. Velocity components and resultant velocity near the pipe wall.

after Blasius's resistance formula which is valid for Reynolds numbers less than 10^5.

When m is taken as 5, the value of α is 0·184. A form of the velocity distribution corresponding to equation (9) may be deduced by means of plausible assumptions [9]. As the result, the velocity distribution is expressed by the $1/(2m-1)$ power law. The Reynolds number Re in equation (9) is calculated by using this velocity distribution. On the other hand, the total shear stress at the wall keeps balance with the pressure gradient. Then, from equation (8) λ is expressed by the stress at the wall τ_w and Re. We can now deduce τ_w from equation (9). In a non-dimensional form this is written as

$$\check{w}^{*2} \equiv \left(\frac{a^2}{\nu^2}\right)\left(\frac{\tau_w}{\rho}\right) = \frac{\alpha}{2^{3+(1/m)}} \times \left[\frac{(2m-1)^2}{m(4m-1)}\right]^{(2m-1)/m} \check{w}_f^{(2m-1)/m}\, \xi_f^{-(1/m)} \tag{10}$$

In order to make the analysis for a curved pipe on the basis of equation (10), the velocity component w in the boundary layer is put in the following form so as to satisfy the boundary conditions:

at

$$\xi = 0, \quad w = 0,$$

and at

$$\xi = \delta, \quad w = w_{1\delta}.$$

$$w = w_{1\delta}(\xi/\delta)^{1/(2m-1)}. \tag{11}$$

The conditions for v are the boundary conditions and the condition of continuity. The boundary conditions are

at

$$\xi = 0, \quad v = 0,$$

and at

$$\xi = \delta, \quad v = v_1.$$

In consideration of the flow field in a cross section shown in Fig. 2, the flow rate of the secondary flow through the plane B–O is to be equal to that through the plane A–B. The condition of continuity is

$$\int_0^\delta v \, d\xi = D(1 - \delta) \sin \psi. \tag{12}$$

So as to satisfy these conditions and follow the $1/(2m - 1)$ power law near the wall, v is written as

$$v = -D \sin \psi \left[-\frac{m}{m-1}\left(\frac{2}{\delta} - 1\right)\left(\frac{\xi}{\delta}\right)^{1/(2m-1)} + \frac{1}{m-1}\left(m\frac{2}{\delta} - 1\right)\left(\frac{\xi}{\delta}\right)\right]. \tag{13}$$

From equation (13) v_f and ξ_f are obtained. Then, w_f is obtained from equation (11).

A friction velocity component in the direction of the pipe axis (θ-direction) is

$$w^{*2} = \frac{w_f}{\breve{w}_f} \breve{w}^{*2} \tag{14}$$

where

$$\breve{w}_f = \sqrt{(v_f^2 + w_f^2)}.$$

Supposing that $v \ll w$, we may write that $\breve{w}_f \approx w_f$. With the aid of equation (11), $\breve{w}_f$ and ξ_f in equation (10) are replaced by $w_{1\delta}$ and δ. Then, equation (14) becomes

$$w^{*2} = \frac{\alpha}{2^{3+(1/m)}} \left[\frac{(2m-1)^2}{m(4m-1)}\right]^{(2m-1)/m} w_{1\delta}^{(2m-1)/m} \delta^{-(1/m)}. \tag{15}$$

In like manner a friction velocity component in the circumferential direction (ψ-direction) is given by

$$v^{*2} = \frac{v_f}{\breve{w}_f} \breve{w}^{*2} \approx \frac{\alpha m}{2^{1+(1/m)}(2m-1)} \times \left[\frac{(2m-1)^2}{m(4m-1)}\right]^{(2m-1)/m} w_{1\delta}^{(m-1)/m} \delta^{-(m+1)/m} D \sin \psi. \tag{16}$$

From equation (7)

$$w_{1\delta} = A + (C/D)(1 - \delta) \cos \psi. \tag{17}$$

It is assumed that C/D is sufficiently small compared with A, and $\delta \ll 1$. Let the power of $w_{1\delta}$ in equations (15) and (16) put in a general symbol M and, the following expansion is made in order to simplify the later calculation, and only the first and second terms in the bracket are taken into account.

$$w_{1\delta}^M = A^M [1 + M(C/AD) \cos \psi + \ldots]. \tag{18}$$

The results obtained finally show that the ratio C/AD is, for example, about 0·4, when $m = 4$. In this case, M in equation (15) is $\frac{7}{4}$. The third term in the bracket of equation (18) becomes

$$\tfrac{1}{2} \times \tfrac{7}{4} \times \tfrac{3}{4}(C/AD)^2 \cos^2 \psi \doteq 0{\cdot}1 \cos^2 \psi.$$

This is reduced to 0·05, when the ψ-averaged effect is considered. Moreover, $(1 - \delta)^2$ is multiplied to this term in the strict expansion. These reasons suggest that the elimination of terms after the third is equivalent to the omission of only a magnitude of a few per cent.

Since both the velocity distribution in the boundary layer and that in the core region are established, the mean velocity in the pipe may be calculated. The dimensionless mean velocity is

$$w_m = (Re/2) = (1/\pi) \left\{ \int_{-\pi}^{\pi} \int_0^{1-\delta} w_1 \eta \, d\eta \, d\psi + \int_{-\pi}^{\pi} \int_0^{\delta} w(1 - \xi) \, d\xi \, d\psi \right\}. \tag{19}$$

The variation of δ with ψ is supposed to be

very small. Hence, δ is replaced by its mean value δ_m.

Substitution of equations (7) and (11) into equation (19) yields the relation between A and δ_m.

$$A = \frac{Re}{2}\frac{1}{1-(1/m)\delta_m + [1/(4m-1)]\delta_m^2}. \quad (20)$$

Now we consider the region bounded by the pipe wall and two cross sections apart by a distance $R\,d\theta$. The equation describing balance of forces exerted upon this portion of fluid is

$$\int_{-\pi}^{\pi}\int_{0}^{a}\frac{\partial p}{R\,\partial\theta} r\,dr\,d\psi = \int_{-\pi}^{\pi}\tau_w a\,d\psi. \quad (21)$$

Use of the dimensionless quantities gives the following relation between C and w^{*2} averaged around the periphery.

$$C = 2w_m^{*2}. \quad (22)$$

Equations (18) and (20) are substituted into equation (15). Then, substitution of equation (15) into equation (22) gives

$$C = \frac{\alpha}{16}\left[\frac{(2m-1)^2}{m(4m-1)}\right]^{(2m-1)/m} Re^{(2m-1)/m} \times \delta_m^{-(1/m)}\left[1+\frac{2m-1}{m^2}\delta_m\right]. \quad (23)$$

Here the terms having magnitudes of order less than δ_m^2 are neglected.

3. *The boundary-layer momentum equations*

The unknown quantities are now reduced to D and δ. They are determined by solving the momentum equations of the boundary layer in the axial and circumferential directions.

The integral equation expressing the equilibrium of momentum in the direction of the pipe axis (θ) is

$$w^{*2} = w_{1\delta}\frac{\partial}{\partial\psi}\int_0^\delta v\,d\xi - \frac{\partial}{\partial\psi}\int_0^\delta vw\,d\xi + C\delta. \quad (24)$$

Equations (7), (11) and (13) are substituted into equation (24). Only the largest terms are taken into account, and δ is replaced by δ_m. Equation (24) becomes

$$w^{*2} = E + F\cos\psi \quad (25)$$

where

$$E = \left[\frac{6m-1}{(2m+1)(4m-1)}\cos^2\psi + \frac{4m(2m-1)}{(2m+1)(4m-1)}\sin^2\psi\right]C, \quad (26)$$

$$F = \frac{6m-1}{(2m+1)(4m-1)}AD. \quad (27)$$

The mean value of equation (25) around the periphery ($\psi = -\pi \sim \pi$) is $C/2$ and satisfies equation (22). The variation of E with ψ is small compared with $F\cos\psi$, so that E is taken as constant and replaced by its mean value $C/2$.

On the other hand, w^{*2} is written in the following form from equation (15)

$$w^{*2} = \frac{C}{2} + \frac{\alpha(2m-1)}{2^{3+(1/m)}m}\left[\frac{(2m-1)^2}{m(4m-1)}\right]^{(2m-1)/m} \times A^{(m-1)/m}C\frac{1}{D\delta_m^{(1/m)}}\cos\psi \quad (28)$$

where the expansion (18) is used.

Since w^{*2} of equation (25) should be identical with that of equation (28), F must be equal to the coefficient of $\cos\psi$ in equation (28). When the largest components of A and C in equations (20) and (23) are substituted, the following relation between D and δ_m is found.

$$D^2\delta_m^{(2/m)} = \frac{\alpha^2(4m^2-1)(4m-1)}{2^7 m(6m-1)} \times \left[\frac{(2m-1)^2}{m(4m-1)}\right]^{[2(2m-1)]/m} Re^{[2(m-1)]/m}. \quad (29)$$

The other relation between D and δ is obtained from the integral equation of momentum in the circumferential direction

$$v^{*2} = -\frac{\partial}{\partial\psi}\int_0^\delta P_\delta\,d\xi - \frac{\sin\psi}{H}\int_0^\delta w^2\,d\xi - \frac{\partial}{\partial\psi}\int_0^\delta v^2\,d\xi + v_1\frac{\partial}{\partial\psi}\int_0^\delta v\,d\xi \quad (30)$$

and the one in the radial direction (η-direction).

$$P_\delta = \int_0^{1-\delta} \frac{w_1^2}{H} \cos\psi \, d\eta - CH\theta. \tag{31}$$

Equation (31) is substituted into equation (30).

The pressure gradient in equation (8) that defines the resistance coefficient λ is expressed non-dimensionally as C given by equation (23). Therefore, for the purpose of obtaining λ it is necessary to know only the mean value of thickness δ. The details about the variation of δ with ψ are not required, if δ_m can be determined without integration of δ with respect to ψ. Hence, a relation between D and δ_m is derived from equations (30) and (31) in the following way.

Equations (7), (11), (13) and (16) are substituted into equations (30) and (31), where the friction velocity v^{*2} is written with the aid of equation (18). When the integrations are carried out, both the right-hand side of equation (30) and v^{*2} are expressed in the form $E' \sin\psi + F'(\cos\psi) \sin\psi$, where E' is constant and $F'(\cos\psi)$ is a function of $\cos\psi$. The terms reduced to the symbol E' relate to the basic relation between the wall shear stress and the driving force of the secondary flow. The equation (30) is understood to consist of the terms E' and the terms $F'(\cos\psi)$ which represent the local deviation of momentum flux from the mean value. The terms $F'(\cos\psi)$ are supposed to determine the deviation of δ from δ_m. In order to obtain δ_m, the terms E are considered. They appear such as

$$v^{*2} \to \frac{m\alpha}{4(2m-1)} \left[\frac{(2m-1)^2}{m(4m-1)}\right]^{(2m-1)/m} \times D\delta_m^{-[(m+1)/m]} Re^{(m-1)/m}$$

$$-\frac{\partial}{\partial\psi}\int_0^\delta P_\delta \, d\xi \to \frac{\delta_m}{4}\frac{Re^2}{H}$$

$$-\frac{\sin\psi}{H}\int_0^\delta w^2 \, d\xi \to -\frac{2m-1}{4(2m+1)}\delta_m \frac{Re^2}{H}.$$

Equating these terms, we have

$$D\delta_m^{-[(2m+1)/m]} = \frac{2(2m-1)}{\alpha m(2m+1)} \times \left[\frac{m(4m-1)}{(2m-1)^2}\right]^{(2m-1)/m} Re^{(m+1)/m}\frac{1}{H}. \tag{32}$$

From equations (29) and (32), D and δ_m are obtained as follows.

$$D = \hat{D} Re^{m/(m+1)} H^{-[1/2(m+1)]} \tag{33}$$

where

$$\log\hat{D} = \frac{1}{m+1}\left[\tfrac{1}{4}\{(2m-1)\log(2m+1) + (18m-5)\log(2m-1) - (10m-1)\log m - (6m-5)\log(4m-1) - (2m+1) \times \log(6m-1) - (14m+5)\log 2\} + m\log\alpha\right] \tag{33'}$$

$$\delta_m = \hat{\delta}_m Re^{-[1/(m+1)]} H^{m/[2(m+1)]} \tag{34}$$

where

$$\log\hat{\delta}_m = \frac{1}{m+1}\{\tfrac{1}{4}\langle 3m\log(2m+1) + (15m-8)\log(2m-1) - (7m-4) \times [\log m + \log(4m-1)] - m\log(6m-1) - 9m\log 2\rangle + m\log\alpha\}. \tag{34'}$$

4. *The resistance coefficient*

The definition of the resistance coefficient for a curved pipe is given by equation (8) when $R\,\partial\theta$ is put in place of ∂Z. By using the non-dimensional quantities we write

$$\lambda_c = \frac{16}{Re^2} C. \tag{35}$$

When equation (23), in which δ_m is given by equation (34), is substituted into equation (35), the following formula for λ_c is obtained.

$$\lambda_c \sqrt{\left(\frac{R}{a}\right)} = \frac{\alpha_c}{[Re\,(a/R)^{(m/2)}]^{1/(m+1)}} \times \left[1 + \frac{\Delta_\lambda}{[Re\,(a/R)^{(m/2)}]^{1/(m+1)}}\right] \tag{36}$$

where

$$\log \alpha_c = \frac{1}{m+1}\{\tfrac{1}{4}\langle -3\log(2m+1) + (16m-7)\log(2m-1) - (8m-3) \times [\log m + \log(4m-1)] + \log(6m-1) + 9\log 2\rangle + m\log\alpha\} \quad (37)$$

$$\log \Delta_\lambda = \frac{1}{m+1}\{\tfrac{1}{4}\langle 3m\log(2m+1) - (15m+4)\log m + (19m-4)\log(2m-1) - (7m-4)\log(4m-1) - m\log(6m-1) - 9m\log 2\rangle + m\log\alpha\}. \quad (38)$$

The formulae for λ_c derived from the commonly used formulae for λ_s in the form of equation (9) are shown in the following paragraphs.

According to the Blasius's formula $\lambda_s = 0{\cdot}316\, Re^{-\frac{1}{4}}$, we put $m = 4$, and for this case we denote λ_s and λ_c by λ_{s4} and λ_{c4} respectively. Since $\alpha = 0{\cdot}316$, equation (10) now becomes

$$\breve{w}^{*2} = 0{\cdot}0233\, \breve{w}_f^{\frac{7}{4}}\, \xi_f^{-\frac{1}{4}}. \quad (39)$$

It may be seen that the expression (39) is in good agreement with experimental data, if the coefficient 0·0233 is modified as 0·0225. Therefore, the value of α equivalent to the modified coefficient, that is 0·305, had better be used in the calculation after equation (10). Hence, in equations (37) and (38), by putting $\alpha = 0{\cdot}305$. Equation (36) becomes

$$\lambda_{c4}\quad \sqrt{\left(\frac{R}{a}\right)} = \frac{0{\cdot}300}{[Re\,(a/R)^2]^{\frac{1}{4}}} \times \left\{1 + \frac{0{\cdot}112}{[Re\,(a/R)^2]^{\frac{1}{4}}}\right\}. \quad (40)$$

This formula agrees well with Ito's empirical formula

$$\lambda_c\sqrt{(R/a)} = 0{\cdot}029 + 0{\cdot}304\,[Re\,(a/R)^2]^{-0{\cdot}25}$$

over the latter's application range $300 > Re\,(a/R)^2 > 0{\cdot}034$.

Ito [7] also made the analysis using the $\frac{1}{7}$ power law, and obtains the result

$$\lambda_c\sqrt{(R/a)} = 0{\cdot}29/[Re\,(a/R)^2]^{\frac{1}{4}}.$$

This formula gives the value 7–8 per cent less than that from his empirical formula. The discrepancy is caused by lack of reasonable consideration of velocity distribution in the boundary layer in Ito's analysis. The latter term in the bracket of equation (40) or (23) is due to the term of (δ_m) in equation (20).

If only w_1 is used to calculate the mean velocity, it is found that $A = Re/2$.

In that case, the velocity profile of the core region is assumed to extend over the whole cross section and the presence of the boundary layer is ignored. In Ito's analysis [7], the relations between the unknown quantities are not given in simple forms, and the complicated procedure of calculation makes it difficult to obtain λ_c in the form of equation (40).

In order to obtain the formula for fairly large Reynolds numbers we put $m = 5$. The formula for a straight pipe is $\lambda_s = 0{\cdot}184\, Re^{-\frac{1}{4}}$. We denote λ_s and λ_c by λ_{s5} and λ_{c5} respectively. The equation (36) becomes

$$\lambda_{c5}\quad \sqrt{\left(\frac{R}{a}\right)} = \frac{0{\cdot}192}{[Re\,(a/R)^{2{\cdot}5}]^{\frac{1}{4}}} \times \left\{1 + \frac{0{\cdot}068}{[Re\,(a/R)^{2{\cdot}5}]^{\frac{1}{4}}}\right\}. \quad (41)$$

A further remark should be written about equation (36). For laminar flow we put $m = 1$. As reported in the previous paper [1], $\lambda_c\sqrt{(R/a)}$ becomes a function of Dean number

$$[Re\sqrt{(a/R)}].$$

We denote λ_c by λ_{c1} in the laminar region.

From equation (36) it is found that λ_c is almost proportional to $(a/R)^{1/2(m+1)}$. As the value of m increases, the difference in radius ratio has still less influence on λ_c. The tendency is shown in Fig. 4. In the present discussion, as a matter of course, cases in which the radius ratio is so large that the state of flow is not so different as the one in a straight pipe and little

importance in engineering applications is found, are excluded.

The bend of a curve indicating the transition from laminar to turbulent flow is written

found that $Re'_s \doteqdot 5{\cdot}0 \times 10^4$. Since $Re' > Re'_s$, equation (43) is not available for R/a larger than 170. For such large R/a, it is recommended to use Re'_s as the lower limit for λ_{c5}. However,

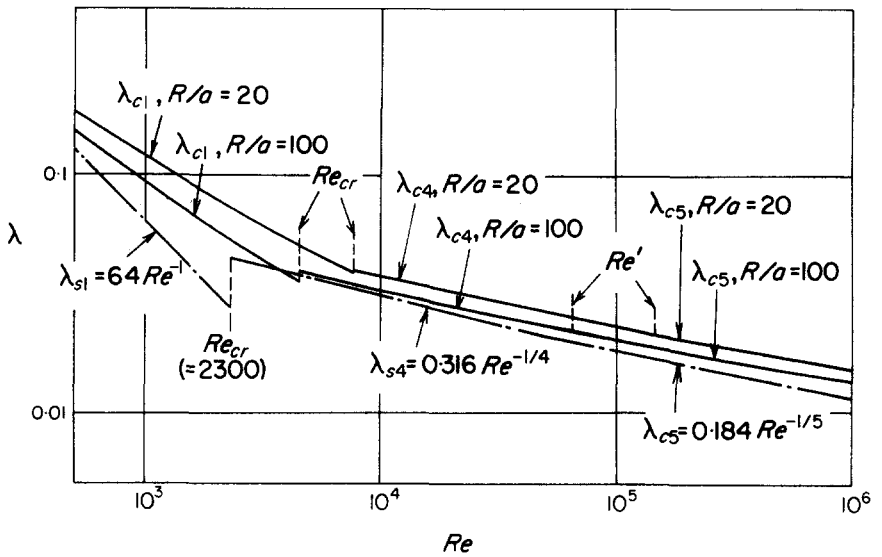

FIG. 4. λ–Re diagram.

according to the Ito's empirical formula for critical Reynolds numbers [7].

$$Re_{cr} = 2 \times 10^4 (a/R)^{0{\cdot}32}. \qquad (42)$$

The Reynolds number at which λ_{c4} comes to exceed λ_{c1} increases, as R/a decreases. This fact seems to imply the same inclination of Re_{cr} as shown in equation (42).

Similar criterion are written for the Reynolds number Re' which defines the lower limit of the application range of λ_{c5}. The real limit is not obvious because of the continuous change of actual λ_c. Therefore, we define it roughly as the Reynolds number at which λ_{c5} comes to exceed λ_{c4}. From equations (40) and (41) it is found that

$$Re' = 6{\cdot}5 \times 10^5 \sqrt{(a/R)}. \qquad (43)$$

If, for a straight pipe, the Reynolds number determined in a similar way is taken to be the critical point for the choice of λ_{s4} or λ_{s5}, it is

because of little difference between λ_{c4} and λ_{c5} in the slope of the curves against Re, the availability of λ_{c4} would fail distinctly at Reynolds numbers far larger than Re' given by equation (43). Usually, it is difficult to make Reynolds number so large in curved pipes. Owing to this reason the experimental data obtained up to the present by many investigators are in good agreement with λ_{c4}. Therefore, equation (40) is convenient enough for practical use.

To illustrate the increase of flow resistance in curved pipes resistance coefficient ratio, λ_c/λ_s, is shown in Fig. 5, λ_{c4} and λ_{s4} being used.

TURBULENT HEAT TRANSFER IN A CURVED PIPE

In the present analysis, the condition of uniform heat flux is defined as meaning that the increasing or decreasing rate of total heat flux through a cross section is constant along the pipe axis. Since the temperature distribution is not symmetrical like that in a straight pipe,

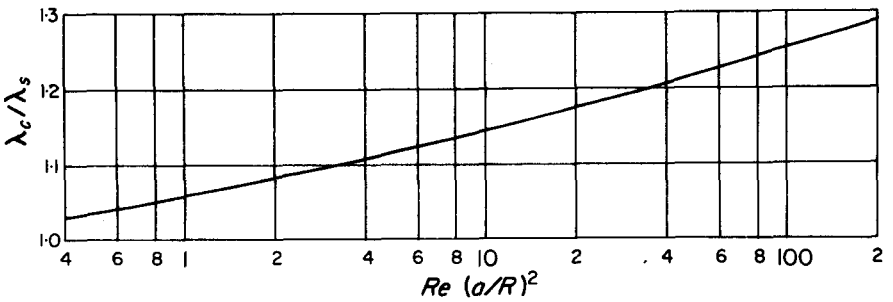

FIG. 5. λ_c/λ_s.

local heat flux from the wall to the fluid may be a function of ψ. This is the same as saying that the ψ-averaged heat flux at the wall is invariable with the distance along the pipe axis ($R\theta$).

For fully developed flow under this condition the time-averaged temperature T can be expressed in the form

$$T = \tau R\theta - G(r, \psi) \tag{44}$$

where τ is a constant temperature gradient along the pipe axis, and $G(r, \psi)$ is a function of r and ψ.

According to Seban and McLaughlin [5], there is a temperature variation around the periphery of a cross section. However, except for fluids having Prandtl numbers considerably less than unity, the Nusselt number for fully developed turbulent flow is hardly affected by the wall temperature condition. This is ascertained by the results for a straight pipe, for example the one given by Seban and Shimazaki [10]. The present purpose is to obtain the Nusselt number averaged around the periphery. Therefore, in the following analysis the wall temperature is assumed to be constant with respect to ψ. Hence, we put

$$T_w = \tau R\theta. \tag{45}$$

Let Q_r, Q_ψ be a heat flux in the r-direction and the ψ-direction respectively, and write

$$q_\eta = \frac{Q_r}{k\tau}, \qquad q_\psi = \frac{Q_\psi}{k\tau},$$

$$g = \frac{G}{\tau a}.$$

When r/R is so small as assumed in the flow field analysis, the energy equation becomes

$$\frac{\partial}{\eta\partial\eta}(\eta q_\eta) + \frac{\partial q_\psi}{\eta\partial\psi} = Pr\, w. \tag{46}$$

Heat fluxes are

$$\left.\begin{aligned} q_\eta &= -\frac{\partial g}{\partial\eta} + Pr\,(ug + \overline{u'g'}) \\ q_\psi &= -\frac{\partial g}{\eta\partial\psi} + Pr\,(vg + \overline{v'g'}) \end{aligned}\right\} \tag{47}$$

where $\overline{u'g'}$, $\overline{v'g'}$ are heat fluxes due to turbulent fluctuation.

The temperature distribution in a pipe is considered to be determined mainly by the effect of the secondary flow like the velocity distribution. The contribution of the secondary flow of heat transfer is supposed to be predominant in the greater part of a cross section. Accordingly, only the terms ug, vg are taken into account in the flow core region.

1. *The temperature field in the core region*

When g in the core region is denoted by g_1, the heat fluxes are

$$q_\eta = Pr\, u_1 g_1, \qquad q_\psi = Pr\, v_1 g_1. \tag{48}$$

Substituting these into equation (46), we find

$$u_1\frac{\partial g_1}{\partial\eta} + v_1\frac{\delta g_1}{\eta\partial\psi} = w_1. \tag{49}$$

The dimensionless temperature g_1 is written in the following form so as to satisfy equation

(49) in which u_1, v_1, and w_1 from equation (7) are substituted.

$$g_1 = A' + (C/2D^2)\eta^2 + (A/D)\eta\cos\psi \quad (50)$$

where A' is a constant.

The constant A' is determined by considering total heat balance about a cylindrical slice of the fluid occupying a cross section of the pipe. It is necessary to know beforehand the relation which creates the local heat flux from the wall to the fluid.

2. *The heat flux at the wall*

When the heat flux at the wall is denoted by Q_w, the non-dimensional heat flux is given by $q_w = Q_w/k\tau$. Interest is now concentrated on the small local portion of the fluid adjacent to the wall. The mechanism of heat transfer in that place is supposed to be the same as that observed in a straight pipe. In other words, when the velocity and the temperature at a given distance from the wall are specified, Q_w is determined by the law applicable to that existing near the wall in a straight pipe. Thus the relation between the non-dimensional variables, q_w, ξ, $\check{w}$ and g is derived from the Nusselt-number formula for a straight pipe.

The formula is usually based on the mixed mean temperature. In order to obtain the local relation, the mixed mean temperature should be disintegrated into the velocity and the temperature. The expression for the temperature distribution in a straight pipe is found in the theoretical paper by Martinelli [11]. However, it is not suitable for the present analysis owing to the rather complicated structure. Hence, we begin with the discussion of a straight pipe.

The Boussinesq expressions for the shearing stress and the heat flux are, in the dimensionless forms,

$$f = \left(1 + \frac{\epsilon}{\nu}\right)\frac{\mathrm{d}\check{w}}{\mathrm{d}\xi} \quad (51)$$

$$q = \left(1 + Pr\frac{\epsilon}{\nu}\right)\frac{\mathrm{d}g}{\mathrm{d}\xi} \quad (52)$$

where ϵ is the eddy diffusivity taken equally for heat and momentum.

The assumption is made that the ratio f/q remains constant in the transverse direction ξ. This assumption is generally used in the elementary theories of turbulent convection. Thus, from equations (51) and (52) the ratio of q_w to the friction velocity is written in the form

$$\frac{q_w}{\check{w}^{*2}} = \frac{\nu + Pr\,\epsilon}{\nu + \epsilon}\frac{\mathrm{d}g}{\mathrm{d}\check{w}}. \quad (53)$$

Near the wall, the coefficient $(\nu + Pr\,\epsilon)/(\nu + \epsilon)$. may be expressed mainly as a function of Prandtl numbers. We divide the flow field into three regions as usual. The regions where the effect of the Prandtl number is important are the laminar sublayer and the buffer layer. In both regions, we reduce the coefficient to the following form

$$\frac{\nu + Pr\,\epsilon}{\nu + \epsilon} = Pr^{1-\gamma_0}. \quad (54)$$

The exponent $(1 - \gamma_0)$ would be chosen for the appropriate range of Prandtl and Reynolds numbers. Hence, equation (53) becomes

$$\frac{q_w}{\check{w}^{*2}} = Pr^{1-\gamma_0}\frac{\mathrm{d}g}{\mathrm{d}\check{w}}. \quad (55)$$

In the turbulent core region, where the effect of turbulent fluctuation is predominant, equation (53) becomes

$$\frac{q_w}{\check{w}^{*2}} = Pr\frac{\mathrm{d}g}{\mathrm{d}\check{w}}. \quad (56)$$

Suppose that the interface between the turbulent core and the buffer layer exists at $\xi = \xi_b$, and denote g, $\check{w}$ at the interface by g_b, $\check{w}_b$ respectively. The integration of equation (55) yields

$$\frac{q_w}{\check{w}^{*2}} = Pr^{1-\gamma_0}\frac{g_b}{\check{w}_b}. \quad (57)$$

From equation (56)

$$g - g_b = \frac{1}{Pr}\left(\frac{q_w}{\check{w}^{*2}}\right)\check{w}_b\left(\frac{\check{w}}{\check{w}_b} - 1\right). \quad (58)$$

When the $1/(2m-1)$ power law is used, the velocity distribution is expressed by

$$(\check{w}/\check{w}_b) = (\xi/\xi_b)^{1/(2m-1)}. \tag{59}$$

Equation (59) is substituted into equation (58) and elimination of (q_w/w^{*2}) from equations (57) and (58) yields g in the turbulent core.

$$g = g_b\{Pr^{-\gamma_0}[(\xi/\xi_b)^{1/(2m-1)} - 1] + 1\}. \tag{60}$$

For the simplicity in calculation, equation (60) is approximated by

$$\check{g} = g_b(\xi/\xi_b)^{(1/n_0)} \tag{61}$$

where

$$n_0 = Pr^{\gamma_0}(2m-1).$$

Comparison between the equation (60) and (61) is shown in Fig. 6 and the above approximation is found to be reasonable.

If we put $\xi = \delta$ in equations (59) and (61), it is found that

$$\check{w}_b = \check{w}_\delta(\xi_b/\delta)^{1/(2m-1)}, \qquad \check{g}_b = \check{g}_\delta(\xi_b/\delta)^{1/n_0}$$

where the suffix δ denotes the value at $\xi = \delta$.

Substituting these into equation (57), we find

$$q_w = Pr^{1-\gamma_0}\check{w}^{*2}(\check{g}_\delta/\check{w}_\delta)(\xi_b/\delta)^{(1/n_0)-[1/(2m-1)]}. \tag{62}$$

When the temperature distribution bears a close resemblance to the velocity distribution, n_0 is nearly equal to $2m-1$, that is, the exponent of (ξ_b/δ) in equation (62) is near zero. Thus q_w depends on the Prandtl number through $Pr^{1-\gamma_0}$ alone. However, this discussion may be allowed in the very limited range of Prandtl numbers about unity. In order to obtain the results applicable in the relatively wide range of Prandtl numbers, we put

$$Pr^{1-\gamma_0}(\xi_b/\delta)^{(1/n_0)-[1/(2m-1)]} = \zeta Pr^{\kappa}. \tag{63}$$

The left-hand side of equation (63) is a function of Pr, δ and Re which determines ξ_b. The coefficient ζ and the exponent κ are constants which should be chosen so as to approximate the true function in the appropriate range of these variables.

The Nusselt number is defined by

$$Nu = \frac{2aQ_w}{k(T_w - T_m)} = \frac{2q_w}{g_m} \tag{64}$$

where g_m is the dimensionless difference between T_w and, the mixed mean temperature, T_m. When the suffix s is used to denote the case of a straight pipe, g_{ms} is given by

$$g_{ms} = (4/Re)\int_0^1 \check{g}\check{w}\,\eta\,d\eta. \tag{65}$$

This is calculated by substitution of equation (61) and $\check{w}$ following the $1/(2m-1)$ power law. Heat flux q_w from equation (62), in which equations (10) and (63) are substituted, and g_{ms} yield the following Nusselt number for a straight pipe.

$$Nu_s = \alpha\zeta\frac{(2m-1)^2(2m+1)}{4m(4m-1)^2}Pr^{\kappa}Re^{(m-1)/m}Y \tag{66}$$

where

$$Y = \left[1 - \frac{6m+1}{4m(2m+1)}(1 - Pr^{-\gamma_0}) + \frac{1}{4m(2m+1)} \times (1 - Pr^{-\gamma_0})^2\right]\delta^{-[1/(2m-1)](1-Pr^{-\gamma})}. \tag{67}$$

In fluids having Prandtl numbers different from unity, the strict analogy between heat and momentum transfer, in the sense usually employed in the elementary theories of turbulent convection, is unlikely to exist. The exponent of Re in the Stanton number formula which is formed by dividing Nu with $Re\,Pr$ is not always identical with that in the resistance formula. When the same amount of q_w is supposed to be given to various fluids, difference in the exponent is caused by the effect of Prandtl numbers on the mixed mean temperature. The temperature distribution is more flattened as the Prandtl number increases. In the present analysis, this contribution of Prandtl numbers is expressed by Y.

The behaviour of Y against Pr^{γ_0} is shown in Fig. 7. It is found that use of large m lessens the

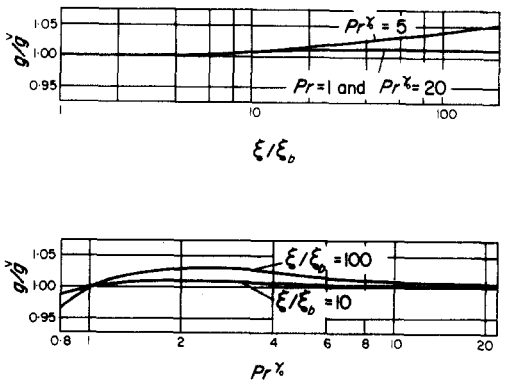

FIG. 6. $g/\check{g}$.

effect of Prandtl numbers. The values of δ represent the order of magnitude of boundary-layer thickness expected in a curved pipe. The case of $\delta = 0{\cdot}1$ is found when $Re\,(a/R)^2 \doteqdot 100$. This is in general the case when Re is very large. For such a large mean velocity region, choice of large m makes the curve of Y come near the line of unity. Moreover, in the region of high Prandtl numbers, if a large value of m is preferred regardless of the magnitude of Re, the deviation of Y from unity can be diminished. For fluids of Prandtl numbers about unity, the value of m should be the same as that in the resistance formula. For other fluids, it is assumed that m in the Nusselt number formula implies the effect of Prandtl numbers, and the value different from that in the resistance formula can be chosen in the Reynolds number region under consideration. With this understanding we put $Y = 1$. As a matter of fact, this assumption is equivalent to the following. Instead of the real temperature and velocity distribution, the one supposed to be the same

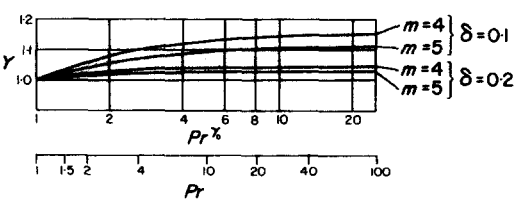

FIG. 7. Y.

for temperature and velocity is considered. This equivalent distribution follows the $1/(2m-1)$ power law. The index m is chosen with the coefficient α from the resistance formula, so as to give the real Nusselt number from equation (66) without Y.

Below the abscissa of Fig. 7 an estimation of Pr against Pr^{γ_0} is shown. The exponent γ_0 is determined to give the agreement between $\check{g}$ from equation (61) and the distribution obtained by Martinelli [11] as shown in Fig. 8. The values of γ_0 are

$$Pr = 1 \sim 1{\cdot}5, \qquad \gamma_0 = \tfrac{2}{3},$$

$$Pr > 1{\cdot}5, \qquad \gamma_0 = 0{\cdot}7.$$

The previous steps relating to heat transfer in a straight pipe are now summarized and applied to the analysis for a curved pipe. The dimensionless temperature difference $\check{g}_\delta$ and the velocity $\check{w}_\delta$ are replaced by $g_{1\delta}$ and $w_{1\delta}$ respectively, where $g_{1\delta}$ is the value of g_1 at $\xi = \delta$. When the Nusselt number for a straight pipe is given in the form

$$Nu_s = \beta\, Re^{(m-1)/m}\, Pr^{\kappa} \tag{68}$$

the local heat flux at the wall q_w in a curved pipe is expressed by

$$q_w = \hat{q}_w\, Pr^{\kappa}\, w_{1\delta}^{(m-1)/m}\, \delta^{-(1/m)}\, g_{1\delta} \tag{69}$$

where

$$\hat{q}_w = 2^{-[(m+1)/m]} \left[\frac{(2m-1)^2}{m(4m-1)}\right]^{(m-1)/m} \times \frac{4m-1}{2m+1}\,\beta. \tag{70}$$

In order to ascertain the relation, Martinelli's results [11] are calculated numerically, and rearranged into the forms of equations (68) and (69) independently. In the region where the Prandtl number is near unity and the Blasius's resistance formula is applicable, Nu_s and q_w are written as follows:

$$Nu_s = 0{\cdot}038\, Re^{\frac{7}{8}}\, Pr^{\frac{1}{3}} \tag{71}$$

$$q_w = 0{\cdot}023\, Pr^{\frac{1}{3}}\, w_{1\delta}^{\frac{7}{8}}\, \delta^{-\frac{1}{8}}\, g_{1\delta}. \tag{72}$$

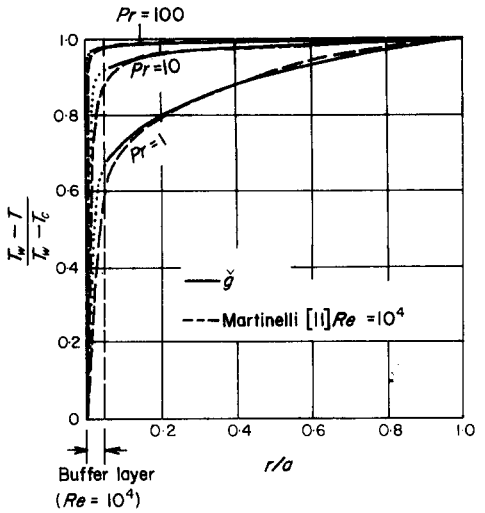

FIG. 8. Comparison of $\check{g}$ with Martinelli's results [11].

On the other hand, when we start with equation (68), we put $\beta = 0{\cdot}038$, $m = 4$ and $\kappa = \frac{1}{3}$ according to the equation (71). It is found that q_w from equations (69) and (70) is the same as that of equation (72).

From equation (50), $g_{1\delta}$ is obtained by putting $\eta = 1 - \delta$. Equation (17) and $g_{1\delta}$ from equation (50) are substituted into equation (69). When the expansion (18) is used, q_w becomes

$$q_w = \check{q}_w Pr^{\kappa} \delta^{-(1/m)} A^{(m-1)/m} \times \left\{ A' + \frac{C}{2D^2} + \frac{m-1}{m} \times \left[\frac{2m(6m-1)}{(4m^2-1)(4m-1)} \right]^{\frac{1}{4}} \frac{A}{D} \cos^2 \psi + \left[\frac{m-1}{m} \left(\frac{2m(6m-1)}{(4m^2-1)(4m-1)} \right)^{\frac{1}{4}} \times \left(A' + \frac{C}{2D^2} \right) + \frac{A}{D} \right] \cos \psi \right\}. \quad (73)$$

3. *Determination of A'*

The portion of fluid bounded by the pipe wall and two cross sections apart by a distance $R\,d\theta$ is considered. The heat balance equation for this control volume is

$$\int_{-\pi}^{\pi} Q_w a\,d\psi = \rho c_p \frac{\partial}{\partial z} \int_{-\pi}^{\pi} \int_{0}^{a} WTr\,dr\,d\psi. \quad (74)$$

This is expressed in the following dimensionless form:

$$q_{wm} = \frac{Re\,Pr}{4} \quad (75)$$

where q_{wm} is the mean value of q_w around the periphery of a cross section.

From equation (73) q_{wm} is obtained

$$q_{wm} = \hat{q}_w Pr^{\kappa} \delta_m^{-(1/m)} A^{(m-1)/m} \times \left\{ A' + \frac{C}{2D^2} + \frac{m-1}{2m} \times \left[\frac{2m(6m-1)}{(4m^2-1)(4m-1)} \right]^{\frac{1}{4}} \frac{A}{D} \right\}. \quad (76)$$

When A, C, D and δ_m given respectively by equations (20), (23), (33) and (34) are substituted into equation (76), A' is determined from equation (75) as follows:

$$A' = (Pr^{1-\kappa} - \Delta_{A'}) \frac{\hat{A}'}{1 + [(m-1)/m^2]\,\delta_m} \times Re^{1/(m+1)} H^{1/2(m+1)} \quad (77)$$

where

$$\Delta_{A'} = \frac{4m(4m-1)(6m-1)}{(4m^2-1)^2} \frac{\beta}{\alpha} \quad (78)$$

$$\log \hat{A}' = \frac{1}{m+1} \{ \tfrac{1}{4} [(4m+7)\log(2m+1) + (4m-7)\log m - \log(6m-1) - 11\log(4m-1) - (8m-15)\log(2m-1) - 9\log 2] + \log \alpha \} - \log \beta. \quad (79)$$

4. *The energy integral equation of the boundary layer*

In the boundary layer, heat transfer due to viscous and turbulent diffusion exists with that caused by the secondary flow. The effect of the former is implied in q_w. The energy integral

equation is written

$$\frac{q_w}{Pr} = g_{1\delta}\frac{\partial}{\partial\psi}\int_0^\delta v\,d\xi - \frac{\partial}{\partial\psi}\int_0^\delta gv\,d\xi + \int_0^\delta w\,d\xi. \quad (80)$$

We put the dimensionless temperature distribution in the boundary layer as

$$g = g_{1\delta}(\xi/\delta)^{1/n} \quad (81)$$

where n is the unknown exponent to be determined from equation (80).

Equations (11), (13) and (81) are substituted into equation (80). When only the largest terms are considered, it is found that the sum of convection terms due to v is equal to q_w/Pr. The contribution of w is neglected, because it has an order of magnitude less than that of the other terms. Performing the integrations in equation (80) yields

$$q_w = \left\{APr\left[\cos^2\psi - \frac{2m}{m-1}\left(\frac{1}{(1/n)+[1/(2m-1)]+1} - \frac{1}{(1/n)+2}\right)\times(\cos^2\psi - \sin^2\psi)\right]\right\} + Pr\,D\left(A' + \frac{C}{2D^2}\right)\times\left[1 - \frac{2m}{m-1}\left(\frac{1}{(1/n)+[1/(2m-1)]} - \frac{1}{(1/n)+2}\right)\right]\cos\psi. \quad (82)$$

We find that the mean value of q_w from equation (82) satisfies the relation given by equation (75). Similar to the analysis of flow field, the terms in the first bracket of the right-hand side are replaced by the mean value of q_w. Equating the coefficient of cos ψ from equations (73) and (82), we find

$$\frac{1}{n} = -\frac{3m-1}{2m-1} + \left[\left(\frac{3m-1}{2m-1}\right)^2 + \frac{4m}{2m-1}\frac{L}{1-L}\right]^{\frac{1}{2}} \quad (83)$$

where

$$L = \frac{4m^2(4m-1)(6m-1)}{(2m-1)^3(2m+1)^2}\frac{\beta}{\alpha}Pr^{-(1-\kappa)} \times \left[\frac{m-1}{m} + \frac{4m(4m-1)^2}{(2m-1)^2(2m+1)} \times \frac{\beta}{\alpha}Pr^{-(1-\kappa)}\right]. \quad (84)$$

When m, α, β and κ are chosen from a Nusselt formula for a straight pipe as shown in the next section, n can be determined. When we put $Pr = 1$,

$$n = 2m - 1. \quad (85)$$

Since the assumption which allows m to imply the effect of Prandtl numbers is introduced in Section 2, the value of n for another Pr seems to lack a reasonable ground. Rather, equation (85) is interpreted as the exponent which gives the equivalent distribution considered in Section 2. Hence, we use equation (85) in calculation of the mixed mean temperature, T_m. It should be noted that rough estimation of T_m is obtained by extending g_1 and w_1 over an entire cross section. When T_m is calculated more precisely, the distribution of g in the boundary layer is used to modify g_1 near the pipe wall. Thus, the exponent n forms a correction term in the Nusselt number formula. Consequently, the variation of n does not have a remarkable effect on Nusselt numbers.

5. *Nusselt numbers*

In equation (64), the dimensionless mean heat flux q_{wm} given by equation (75) is put in place of q_w. Then, the Nusselt number in a curved pipe Nu_c is written,

$$Nu_c = \frac{2q_{wm}}{g_m} = \frac{Re\,Pr}{2g_m} \quad (86)$$

where

$$g_m = \frac{2}{\pi\,Re}\left[\int_{-\pi}^{\pi}\int_0^{1-\delta} g_1 w_1\,\eta\,d\eta\,d\psi\right.$$

$$+\int_{-\pi}^{\pi}\int_{0}^{\delta} gw(1-\xi)\,d\xi\,d\psi\Bigg]. \qquad (87)$$

Using all the knowledge obtained about the temperature and velocity field, we may calculate equation (87) by the order of magnitude δ. Equation (86) becomes

$$Nu_c = \frac{1}{2\hat{A}'}\frac{Pr}{Pr^{1-\kappa}-\Delta g_m} Re^{m/(m+1)} \times \left(\frac{a}{R}\right)^{1/[2(m+1)]}\left\{1+\frac{\Delta_{Nu}}{[Re\,(a/R)^{m/2}]^{1/(m+1)}}\right\} \qquad (88)$$

where $\hat{A}'$ is given by equation (79), and

$$\Delta g_m = \frac{4(6m-1)(4m-1)\,m(m-1)}{(2m+1)^2(2m-1)^3}\frac{\beta}{\alpha} \qquad (89)$$

$$\Delta_{Nu} = \frac{4m^2-2m-1}{m^2(2m+1)}\hat{\delta}_m. \qquad (90)$$

The coefficient $\hat{\delta}_m$ is obtained from equation (34'). If we take equation (71), we have

$$\beta = 0{\cdot}038, \qquad \kappa = \tfrac{1}{3}, \qquad m = 4.$$

The equivalent resistance formula is λ_{s4} given by Blasius. The modified value of coefficient, $\alpha = 0{\cdot}305$, is employed as in the derivation from the resistance formula to calculate Nu_c. In this case equation (88) becomes

$$Nu_c = \frac{Pr}{26{\cdot}2(Pr^{\frac{2}{3}}-0{\cdot}074)} \times Re^{\frac{1}{2}}\left(\frac{a}{R}\right)^{\frac{1}{10}}\left\{1+\frac{0{\cdot}098}{[Re\,(a/R)^2]^{\frac{1}{4}}}\right\}. \qquad (91)$$

This formula agrees well with the experimental results for air as shown in Fig. 9. In the figure, the experimental data, the theoretical curve for laminar air flow in the region of large Reynolds numbers, which is drawn from the curves for first and second approximation [1], and Nu_s given by equation (71) are also shown.

For gases, of which Prandtl numbers are in the neighbourhood of unity, the conclusive discussion of resistance coefficients may be applied to the Nusselt number formula. Namely, the applicability of equation (91) obtained by putting $m = 4$ remains well except for extremely large Reynolds number. Equation (91) seems to be available for practical use.

Most of the experimental data for water are arranged into the form $Nu_c\,Pr^{-0{\cdot}4}$ [4–6]. This form is introduced from the following conventional formula for a straight pipe.

$$Nu_s = 0{\cdot}023\,Re^{0{\cdot}8}\,Pr^{0{\cdot}4}. \qquad (92)$$

If the derivation of Nu_c is based on equation (92),

$$\beta = 0{\cdot}023, \qquad m = 5, \qquad \kappa = 0{\cdot}4.$$

When these values are used, $Pr^{1-\kappa}/(Pr^{1-\kappa}-\Delta g_m)$ in equation (88) comes near unity for large Pr as shown in Fig. 10. Therefore, in the range of large Prandtl numbers, it is convenient to put

$$\frac{Pr^{1-\kappa}}{Pr^{1-\kappa}-\Delta g_m} \approx 1 \qquad (93)$$

for the simplicity of calculation, and for direct comparison with the empirical formulae suggested by some experimenters [4–6].

It must be noted that this approximation more or less compensates for the over estimation caused by putting $Y = 1$ in equation (66). In the derivation of Nu_s from q_w, assumption of $Y = 1$ causes underestimation of Nu_s. It is conversely written that q_w given by equation (69) may be larger than the value equivalent to Nu_s from equation (68), and gives a slightly higher value of Nu_c. Thus, we may write the Nusselt number formula for liquids which have in general high Prandtl numbers as follows:

$$Nu_c\,Pr^{-0{\cdot}4} = \frac{1}{41{\cdot}0}Re^{\frac{5}{6}}\left(\frac{a}{R}\right)^{\frac{1}{12}} \times\left\{1+\frac{0{\cdot}061}{[Re\,(a/R)^{2{\cdot}5}]^{\frac{1}{4}}}\right\}. \qquad (94)$$

Equation (94) is compared with the empirical formulae in Figs. 11 and 12. The empirical correlations are listed below.

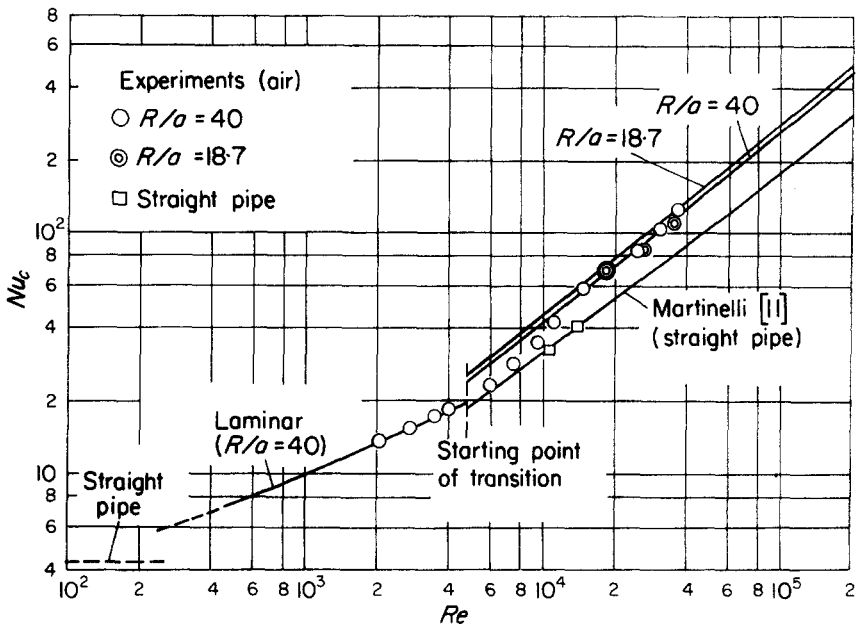

FIG. 9. The theoretical curves for Nu_c and the experimental results.

Pratt [4]:

$$Nu_c\, Pr_b^{-0.4} = 0.0225\,(1 + 3.4\, a/R)\, Re_b^{0.8}. \quad (95)$$

Seban and McLaughlin [5]:

$$Nu_c\, Pr_f^{-0.4} = 0.023\,(a/R)^{0.1}\, Re_f^{0.85}. \quad (96)$$

Rogers and Mayhew [6]:

$$Nu_c\, Pr_f^{-0.4} = 0.021\,(a/R)^{0.1}\, Re_f^{0.85} \quad (97)$$

$$Nu_c\, Pr_b^{-0.4} = 0.023\,(a/R)^{0.1}\, Re_b^{0.85}. \quad (98)$$

The suffixes b and f denote evaluation of physical properties at bulk (mixed mean) and film temperatures respectively.

The Reynolds number exponent of 0·85 used in equations (96–98) is in the vicinity of the present result $\frac{5}{6}(= 0.833\ldots)$. The difference in the radius ratio exponent does not have a significant effect on Nu_c, because in any formula it is very small. Bearing in mind the accuracy of experiments, we may conclude that equation (94) agrees well with the experimental results.

From equations (68) and (88), the ratio of Nu_c to Nu_s is expressed as

$$\frac{Nu_c}{Nu_s} = \frac{Pr^{1-\kappa}}{2\hat{A}'\beta\,(Pr^{1-\kappa} - \Delta g_m)} \times \left[Re\left(\frac{a}{R}\right)^{m/2}\right]^{1/[m(m+1)]} \times \left\{1 + \frac{\Delta_{Nu}}{[Re\,(a/R)^{m/2}]^{1/(m+1)}}\right\}. \quad (99)$$

The values of m and α used up to now are given to equation (99). Figure 13 and Fig. 14 show the increase of Nusselt numbers for gases and liquids respectively. Though many formulae for Nu_s are suggested, Fig. 14 would be available for rough estimation of Nu_c for any kind of liquid. However, the experimental data for oil have not been fully established. The absence of data is due to difficulties in making viscous oil turbulent especially in a curved pipe where transition from laminar to turbulent occurs at higher velocity than in a straight pipe.

Equation (99) shows that the difference

between Nu_c and Nu_s decreases slightly as Pr becomes large. This behaviour is in contrast with the results for laminar flow [1]. The opposite inclination is caused by the difference in mechanisms of heat transfer which can be seen in the formula of Nu_s for laminar flow ($Nu_s = \frac{48}{11}$) and for turbulent flow ($Nu_s \propto Pr^{\kappa}$).

Similar discussion to that about λ_c can be made from equation (88) or (99). As the value of m to be applied becomes large, the difference in R/a has less influence on Nu_c.

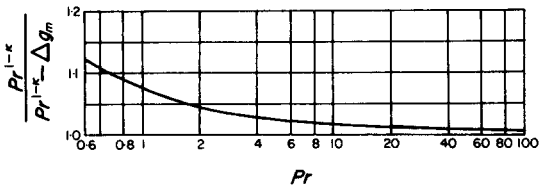

FIG. 10. $Pr^{1-\kappa}/(Pr^{1-\kappa} - \Delta g_m)$.

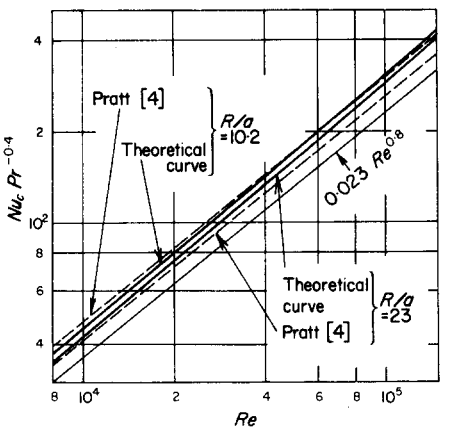

FIG. 11. Comparison of the theoretical results with the empirical formula [4].

EXPERIMENTS

Experimental investigation in air flow was done on two cases of radius ratio, 40 and 18·7. The pipes were heated by nichrom wires wound around them. The heating wires were divided into several sections along the pipe axis. By adjusting electrical power input to these sections, a constant wall temperature gradient along the pipe axis was maintained. The velocity and temperature distributions inside the pipe were measured by inserting probes through little access holes at the pipe wall far downstream of the inlet. One of the measured distributions is shown in Fig. 15. The profiles show a steep gradient of velocity and temperature near the pipe wall. The presence of the boundary layer is ascertained.

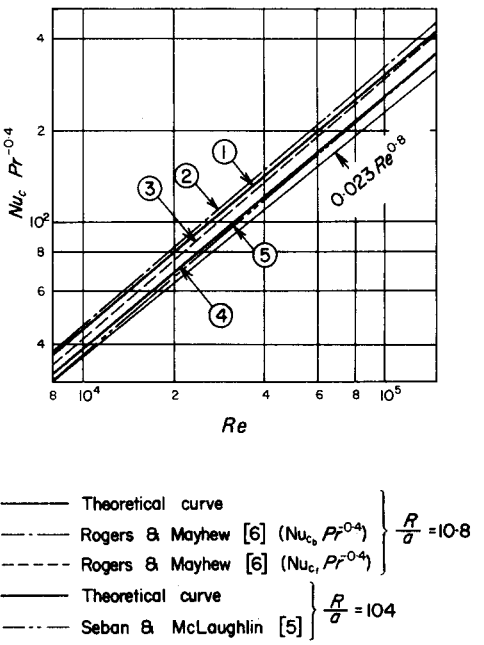

FIG. 12. Comparison of the theoretical results with the empirical formulae [5, 6].

The detailed description of the experimental apparatus is given in the previous paper [1]. The curved pipe of $R/a = 40$ is the same as that used for laminar flow case [1].

The pipe of $R/a = 18{\cdot}7$ is of steel and has the following dimensions:

Inside diameter	$2a = 53{\cdot}6$ mm
Wall thickness	3·5 mm
Radius of curvature	$R = 500$ mm
Angle of θ between the inlet and the outlet	300 degrees.

A cross section of the pipe does not form a

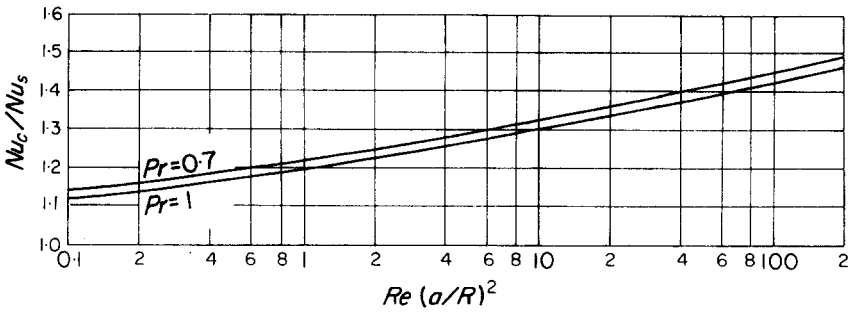

FIG. 13. Nu_c/Nu_s for gases ($Pr \approx 1$).

complete circle because of distortion caused by bending. Difference between the maximum outside diameter and the minimum diameter at a cross section is 2 ~ 3 mm. The inside diameter is obtained by converting a cross sectional area, which was found by cutting a test piece from the pipe, to an area of a circle. This equivalent diameter differs about 1 per cent from the original diameter prior to bending.

Cu–Co thermocouples for measurements of the wall temperature were buried in the wall to the depth of 2 mm from the surface. The temperature drop due to conduction through the wall was taken into account, but the correction gave little change on measured T_w. The thermocouples are located at 9 stations at intervals of 30 degrees in θ. The velocity and temperature distributions were measured at $\theta = 150°$ and 210° (the inlet of the curved pipe section is at $\theta = 0°$). The distribution profiles are found to be similar to those for $R/a = 40$.

For both cases of radius ratio, wall temperature variation around the periphery of a cross section was checked at two stations by attaching four thermocouples at the top, bottom, inner and outer side of the wall. (The curved pipe is placed so as to let the centre of curvature and the pipe axis be in a horizontal plane.) The wall temperature T_w used in plotting the temperature distribution and calculating the Nusselt number is the mean value around the periphery. The deviations from the mean value are, for example, +1·35°C at the inner side, −1·15°C at the outer side, +0·05°C at the top and −0·25°C at the bottom when the mean wall temperature = 44·15°C, $T_m = 24·6$°C, $\tau = 6·2$°C/m, $Re = 3·6 \times 10^4$, $R/a = 18·7$. It was found that evaluation of T_w at a fixed peripheral location introduces an error of several per cent at worst in Nu_c. However, this example is the worst one. The variations found throughout the experiments for $R/a = 40$ are far below the above example.

From the esperiments, Nusselt numbers are obtained by the method shown in the previous paper [1]. The rough description of the method is given here. Mean heat flux at the wall Q_{wm} is written from equation (74)

$$Q_{wm} = \tfrac{1}{4}\tau k\, Re\, Pr. \qquad (100)$$

Therefore, the wall temperature gradient τ obtained from the measured wall temperature distribution gives Q_{wm}. The velocity and temperature distributions on a horizontal line are assumed to have similar profiles to those obtained by transversing through the centre of a cross section. Both distributions extended over a whole cross section are utilized to multiply numerically temperature by velocity dividing the cross section into small parts. Thus, the mixed mean temperature T_m is computed. The physical properties are evaluated at T_m. The results are shown in Fig. 9. The data for $R/a = 40$ agree well with the theoretical curve of a fully turbulent region. The data for $R/a = 18·7$ at $Re = 2·7 \times 10^4$

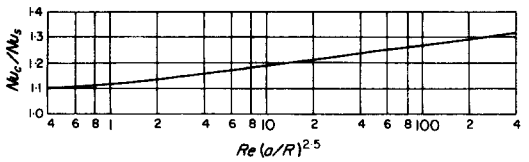

FIG. 14. Nu_c/Nu_s for liquids ($Pr > 1$).

and $3{\cdot}6 \times 10^4$ are found to be below the analytical result. In these cases a little irregular temperature rise along the pipe axis (θ) caused inaccuracy in determining Q_{wm}. The experimental point at $Re = 1{\cdot}9 \times 10^4$ is obtained by determination of τ from fluid temperature rise which was measured by inserting the thermocouple probe at several stations along the pipe axis. The same method for obtaining Nusselt numbers experimentally was applied in the case of the straight pipe. The straight pipe is of brass and 35·6 mm in diameter. The velocity and temperature distributions were measured in the region where both profiles were fully developed and the effect of buoyancy was negligibly small. The results are shown in Fig. 9 and are in good agreement with Nu_s given by equation (71).

CONCLUSIONS

Turbulent flow and temperature field in a curved pipe fully developed under the condition of constant heat flux were analysed by theory and experiment, and the following conclusive results were obtained.

(1) The theoretical analysis of a flow field was done by assuming a thin boundary layer along the pipe wall. Frictional stress at the wall was derived from the resistance formula for a straight pipe expressed by $\lambda_s \propto Re^{-1/m}$. The result shows that the resistance formula for a curved pipe is given in the form of $\lambda_c\sqrt{(R/a)}$ which is a function of $Re\,(a/R)^{m/2}$. One of the resistance formulae is obtained by putting $m = 4$ according to the Blasius's formula for λ_s and taking into account not only the velocity profile of a flow core occupying the greater part of a cross section but also that of the boundary layer. The formula agreed well in a fairly wide range of $Re\,(a/R)^2$ with Ito's empirical formula [7] which summarizes the data of many investigators.

(2) The analysis of heat transfer was done by deriving heat flux at the wall from the Nusselt

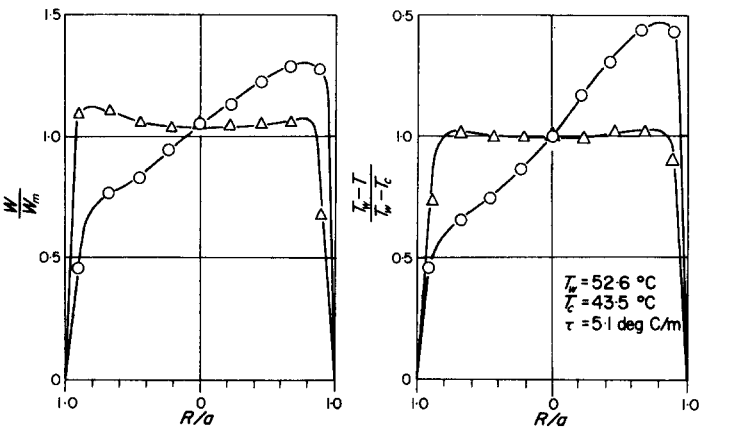

FIG. 15. The velocity and temperature distributions ($R/a = 40$, $Re = 2{\cdot}5 \times 10^4$).

number formula for a straight pipe expressed by $Nu_s \propto Re^{(m-1)/m} Pr^{\kappa}$. The general expression of the Nusselt number for a curved pipe Nu_c was obtained. The ratio Nu_c/Nu_s is expressed as a function of $Re\,(a/R)^{m/2}$ and Pr.

The formula for gases ($Pr \approx 1$) given by putting $m = 4$ is in good agreement with the experimental data of air. The formula for liquids ($Pr > 1$) expressed in the form of $Nu_c\,Pr^{-0.4}$ by putting $m = 5$ agreed with the empirical formulae suggested by some experimenters [4–6].

Figure 13 and Fig. 14, showing Nu_c/Nu_s, might be available for rough estimation of Nu_c though a different formula of Nu_s is to be applied appropriately to various cases.

(3) When flow is turbulent, λ_c and Nu_c do not show such a remarkable increase from λ_s and Nu_s as found in laminar flow [1]. The value of m is to be chosen in the appropriate range of Re and Pr. As Re or Pr increases, the value of m to be used becomes larger, so that the difference in R/a has less influence on λ_c and Nu_c.

(4) Experimental investigation in air flow was done in two cases of $R/a = 40$ and 18·7. The velocity and temperature distributions in the pipe were measured keeping the wall temperature gradient along the pipe axis constant. Applicability of the boundary layer approximation was ascertained by the measured distributions. The Nusselt numbers obtained experimentally agreed well with the theoretical result.

REFERENCES

1. Y. MORI and W. NAKAYAMA, Study on forced convective heat transfer in curved pipes (1st report, laminar region), *Int. J. Heat Mass Transfer* **8**, 67–82 (1965).
2. D. JESCHKE, Wärmeübergang und Druckverlust in Rohrschlagen, *Z. Ver. Dt. Ing.* **69**, 1526 (1925); *Z.V.D.I.* **24**, 1 (1925).
3. W. H. MCADAMS, *Heat Transmission*, p. 228. McGraw-Hill, New York (1954).
4. N. H. PRATT, The heat transfer in a reaction tank cooled by means of a coil, *Trans. Instn Chem. Engrs* **25**, 163–180 (1947).
5. R. A. SEBAN and E. F. MCLAUGHLIN, Heat transfer in tube coils with laminar and turbulent flow, *Int. J. Heat Mass Transfer* **6**, 387–395 (1963).
6. G. F. C. ROGERS and Y. R. MAYHEW, Heat transfer and pressure loss in helically coiled tubes with turbulent flow, *Int. J. Heat Mass Transfer* **7**, 1207–1216 (1964).
7. H. ITO, Friction factors for turbulent flow in curved pipes, *J. Bas. Engng* **81**, 123–134 (1959).
8. M. ADLER, Strömung in gekrümmten Rohren, *Z. Angew. Math. Mech.* **14**, 257–275 (1934).
9. S. GOLDSTEIN, *Modern Developments in Fluid Dynamics*, p. 339. University Press, Oxford (1957).
10. R. A. SEBAN and T. T. SHIMAZAKI, Heat Transfer to a fluid flowing turbulently in a smooth pipe with walls at constant temperature, *Trans. Am. Soc. Mech. Engrs* **73**, 803–809 (1951).
11. R. C. MARTINELLI, Heat Transfer to Molten Metals, *Trans. Am. Soc. Mech. Engrs* **69**, 947–959 (1947).

Résumé—L'effet de la courbure sur le transport de chaleur à flux de chaleur constant pour un écoulement turbulent entièrement établi dans des tuyaux courbes a été étudié théoriquement et expérimentalement. On suppose dans l'analyse qu'il existe une couche limite le long de la paroi du tuyau. La contrainte de cisaillement locale et le flux de chaleur local à la paroi sont donnés dans but de réduire les formules du coefficient de perte de charge linéique (λ_s) et du nombre de Nusselt (Nu_s) à la relation locale du frottement et du transport de chaleur. Lorsque les formules pour les tuyaux rectilignes sont de la forme $\lambda_s \propto Re^{-1/m}$ et $Nu_s \propto Re^{(m-1)/m}$, on montre que la similitude dynamique et la similitude pour le transport de chaleur dans les tuyaux courbes dépendent de $Re\,(a/R)^{m/2}$.

Le coefficient de perte de charge linéique et le nombre de Nusselt pour les tuyaux courbes sont obtenus en posant $m = 4$ ou $m = 5$.

Les nombres de Nusselt obtenus à partir des mesures des distributions de vitesse et de température dans un écoulement d'air à travers des tuyaux courbes tels que $R/a = 40$ et 18,7 sont en bon accord avec les résultats théoriques.

Zusammenfassung—In dieser Arbeit wird der Einfluss der Krümmung auf den Wärmeübergang für ausgebildete turbulente Strömung in gekrümmten Rohren bei konstanter Wärmestromdichte theoretisch und experimentell untersucht. Der Analyse wird eine Grenzschicht entlang der Wand zugrundegelegt. Die örtliche Schubspannung und die örtliche Wärmestromdichte werden angegeben um den Widerstand (λ_s) und die Nusselt-Zahl (Nu_s) für gerade Rohre auf die örtlichen Beziehungen für Reibung und Wärmeübergang zurückzuführen. Werden die Gleichungen für gerade Rohre mit $\lambda_s \sim Re^{-1/m}$ und $Nu_s \sim Re^{(m-1)/m}$ angegeben, so kann gezeigt werden, dass die dynamische Ähnlichkeit und die Ähnlichkeit des

Wärmeübergangs in gekrümmten Rohren abhängig ist von $Re(a/R)^{m/2}$. Der Widerstandskoeffizient und die Nusseltzahl für gekrümmte Rohre lassen sich erhalten wenn man $m = 4$ oder $m = 5$ setzt.

Die Nusselt-Zahlen, die durch Messungen der Geschwindigkeitsund Temperaturverteilungen in einem Luftstrom durch gekrümmte Rohre von $R/a = 40$ und 18,7 erhalten wurden, stimmen gut mit theoretischen Ergebnissen überein.

Аннотация—В работе проводится экспериментальное и теоретическое исследование влияния кривизны на теплообмен в полностью развитом турбулентном течении в искривленных трубах при постоянном тепловом потоке. При анализе принимается существование пограничного слоя на стенках трубы. Локальные напряжения трения и локальный тепловой поток рассчитаны из формул сопротивления (λ_s) и числа Нуссельта (Nu_s) для прямых труб, приведенных к соотношениям локального трения и теплообмена. Показано, что в то время как формулы для прямых труб даются в виде $\lambda_s \propto Re^{-1/m}$ и $Nu_s \propto \mathrm{Re}^{(m-1)/m}$, динамическое и тепловое подобие искривленных труб зависит от $Re(a/R)^{m/2}$. Получены коэффициенты сопротивления и числа Нуссельта для искривленных труб при $m = 4$ и $m = 5$.

Числа Нусскльта, полученные при измерении профилей скорости и температуры при течении воздуха в искривленных трубах при $R/a = 40$ и 18,7, хорошо согласуются с теоретическими.